International Journal of Refractory Metals and Hard Materials (2014).
DOI: http://dx.doi.org/10.1016/j.ijrmhm.2014.09.030

Cermets based on FeAl-NbC from composite powders: design of composition and processing

Eliana Franco[a,*], César Edil da Costa[a], Sophia Alexandra Tsipas[b], Elena Gordo[b]

[a]Department of Mechanical Engineering, Universidade do Estado de Santa Catarina, Rua Paulo Malschitzki, s/n, CEP 89219-710, Joinville, Brazil
[b]Department of Materials Science and Engineering, Universidad Carlos III de Madrid, IAAB, Avda. Universidad, 30, E-28911 Leganés, Spain
∗ Corresponding author. Tel.: +55 4734272762,
E-mail address: eliana_franco@globo.com (Eliana Franco).

ABSTRACT

The aim of this work is the design, processing and characterization of a metal–ceramic composite (cermet) with an iron – aluminum alloy as metallic matrix and NbC as ceramic phase. The cermet is obtained from a composite powder containing in situ formed NbC-rich precipitates on an iron rich metal matrix. The starting powder was supplied by CBMM (Brazil), and it was produced by a synthesis process under development which introduces other metals such as Al, Si and Ti to the composition. Due to the in situ process, good bonding is expected between the carbide and the matrix. However it is necessary to study the processability of those complex particles and the transformations occurring during sintering to get the final microstructure. Thermodynamic studies by means of ThermoCalc® software were performed to predict the phases stable with the starting composition and also the influence of Fe and C additions. Samples were produced by uniaxial pressing and vacuum sintering (PS), and also by Field Assisted Hot Pressing (FAHP). The processing parameters for PS processing, that is, sintering temperature and time were based on themodynamic simulations by ThermoCalc® software together with thermal analysis. The powders were characterized by measuring density, particle size, carbon content and chemical composition; and consolidated samples by density and Vickers hardness. The microstructure and morphology of the powder and consolidated samples was analyzed by SEM. The addition of Fe and both C and Fe to the starting cermet composition provided good results as the final microstructure consisted essentially of NbC and Fe matrix.

Abbreviations
PS – Pressing and Sintering
FAHP – Field Assisted Hot Pressing

Keywords: FeAl-cermets; NbC in situ; powder metallurgy; thermal analyses; ThermoCalc®

1. Introduction

Cermets are composite materials constituted by a ceramic phase, typically formed by carbides or carbonitrides of refractory metals, bonded by a metallic phase typically Ni or Co. These materials have many applications as wear parts for cutting and forming [1], [2]. There is an increasing interest in the total or partial replacement of Co and Ni as metallic matrix as these are scarce and cause environmental and health problems. For instance, Ni-based powders come under the H351 hazard statement according to European Commission regulation EC 790/2009 [3]. WC–Co materials are also toxic by inhalation and are currently under consideration for inclusion in the list of suspect human carcinogens as well [4].

The use of iron as metallic phase presents several advantages over Co or Ni, including non-toxicity, abundance of resources leading to lower cost and the ability to be hardened by heat treatment, which could lead to a high hardness with a lower quantity of ceramic phase [5]. However, Fe-based cermets present low sintering performance due to the poor wettability of the liquid phase and the risk of reaction with the ceramic phase that can lead to embrittlement [6]. Several cermets based on iron have proved to have good wear resistance. Fe alloys-based cermets with TiC as reinforcement demonstrated their noticeable superiority over Ni alloys-based cermets with TiC in wear conditions with prevalence of adhesion [7]. The cermet formed by high-speed steel M2 with 50% vol. of TiCN showed improved wear resistance and increased tool life when compared with both the reference material M2 sintered at the laboratory and the commercial HSS inserts in turning by dry cutting operations [8].

Regarding the hard phase, the element of wider application among the transition metals of the groups IVB to VIB in the periodic table to form extremely hard carbides and nitrides is W in the form of WC, and its most significant application is on hard metals for cutting tools. Nevertheless, nowadays significant increase in labor cost escalated the prices for tungsten [9].

Additions in small amounts (0.25 to 3.0 wt. %) of vanadium carbide, tantalum carbide, niobium carbide or chromium carbide are commonly used in hard metals to inhibit the grain growth, being the VC the most efficient. The addition of these carbides also improves the processing by improving the wettability between the ceramic and the liquid phase, as well as enhancing the density [10], [11]. These hard metals with additions are known as complex grades, multigrades, or steel-cutting grades [12]. The addition of TaC often occurs along with NbC because the chemical similarity between these two elements makes their separation expensive, furthermore niobium carbide has an effect similar to tantalum carbide in most cases [12]. Niobium carbide is resistant to wear and corrosion and retains these properties at high temperatures, its hardness is in the range of 2400 HV and the melting temperature is 3420^{o} C [13]. This carbide can compete in wear resistance with reference materials such as WC, Cr_3C_2, (Ti, Mo)(C,N) [9].

However, niobium carbide was hardly used in technical applications to date, and this may be associated with its late discovery, as niobium became available only after pyrochlore reserves were developed in Brazil and Canada during the 1960's [14]; with its poor sintering ability, which can today be overcome by hot pressing, high-frequency inductive heated sintering or by spark-plasma sintering; and moreover with its high cost, despite the interesting properties of NbC, this material is still too expensive to be used as a major ceramic phase in cermets [15].

Combining the advantages of Fe alloys for the metal matrix with the interesting properties of NbC would lead to competitive materials for some tool applications. The manufacturing of Fe- NbC based composite materials is normally done by techniques based on the addition of NbC particles to the metal matrix in molten or powder form [16]–[19]. In such cases, the amount of reinforcing phase NbC is limited by the size of the starting powder, interfacial reactions between reinforcements and matrix and by the poor wettability between the reinforcements and the matrix due to surface contamination of the reinforcements. Moreover, the bonding strength of NbC particles with the Fe matrix is usually poor [20]. The obtaining of these cermets has also been developed by other routes, such as by the addition of Nb to molten gray iron to form in situ carbides [20]; the mechanosynthesis [21]; and the self-propagating high temperature synthesis (SHS) [22]. A small particle size results in improved properties of the material produced. The cermet produced by adding Nb to the molten gray iron formed particles of size 0.3-3.5 μm, presenting hardness of 286 $HV_{0.05}$ with a content of approximately 30 wt.% of NbC in the matrix and wear resistance 5.9-fold higher than that of the gray cast iron under a 20N load [20]. In mechanosynthesis, the size of the powder particles ranged from 0.3 to 50 μm. This

cermet was compacted by magnetic pulse compaction showing a hardness of 1224 HV with about 30 wt. % NbC [21]. By SHS, a composite was obtained formed by NbC precipitates in an Fe matrix; the maximum particle size of the powder obtained was 300 μm, reaching a size of 4 μm after high energy milling [22]. After uniaxial compression at 700 MPa and sintering under vacuum at 1450 C for 60 min, this cermet presented hardness of 800 HV, with 70 wt. % NbC [22]. For comparison purposes, a cermet composed by a high-speed steel matrix (grade M2) with 50 vol.% Ti(C,N) particles of size about 4μm, after uniaxial pressing and vacuum sintering at 1400ºC had a hardness of 1336 HV [23].
The aim of this work is the design, processing and characterization of an iron-based cermet with NbC particles as hard phase. The powder used as raw material is obtained by reaction of the Nb ore with elements such as Fe, Al and Ti, to form niobium carbides in-situ in a metallic matrix. Due to the synthesis method for the extraction of niobium carbides a good bond is expected between the metallic and ceramic phases, as well as a good distribution of phases.

2. Experimental procedure

The starting material, from now on referred to as Fe10Al-NbC, is a composite powder supplied by CBMM consisted of NbC-rich precipitates embedded in a Fe-rich metal matrix containing also Al, Si and Ti from the extraction process. This powder needed to be fully characterized as it is not a commercial powder. The characterization consisted on measuring density in a He pycnometer Micromeritics Accupyc 1330, particle size distribution by laser diffraction in a Mastersizer 2000 of Malvern Instruments, UK, carbon content by combustion infrared detection in a CS-200 LECO equipment, and chemical composition by X-ray fluorescence in a Shimadzu EDX-700 equipment. The phases and microstructure of the powder particles were analyzed by X-Ray Diffraction (XRD) in a Philips X'Pert diffractometer and by Scanning Electron Microscopy (SEM) in a Philips XL 30 microscope equipped with EDS microanalysis. X-Ray diffraction was carried out with Cu radiation (λ=1.5405), current of 40 mA, accelerating potential of electrons of 40 kV. The scan was performed for angles 2 theta between 20 and 85 degrees, time per step of 0.8. To identify the diffraction peaks of the materials analyzed the PCPDFWIN database was used.
The composite powder was consolidated by conventional powder metallurgy (cold uniaxial pressing and sintering, PS) and by FAHP (Field Assisted Hot Pressing) to obtain a reference material, but also the composition was modified by addition of C and Fe. The C addition is to promote the complete reaction with Nb to form NbC and avoid the formation of the intermetallics. The amount of carbon added was calculated to obtain the stoichiometric NbC, resulting in addition of 1.2 wt% C to obtain the cermet named Fe10Al-NbC+C. To increase the amount of metallic matrix up to 50 wt.% Fe carbonyl powder was added and this material was named Fe10Al-NbC+Fe. Finally, the cermet Fe10Al-NbC+C+Fe was designed to obtain stoichoimetric NbC in a 50 wt% Fe matrix. The compositions prepared and studied are summarized in Table 1, showing the total amount of C and Fe.

Table 1. Content of C and Fe in the compositions prepared and studied.

Cermet designation	**Addition (wt. %)**		**Total amount in the final composition (wt. %)**	
	C	**Fe**	**C**	**Fe**
Fe10Al-NbC	-	-	4.8	36.5
Fe10Al-NbC+C	1.2		6.0	36.1
Fe10Al-NbC+Fe		21.7	3.9	47.8

Fe10Al-NbC+C+Fe	1.2	19.4	4.9	46.4

The processing parameters for PS processing, that is, sintering temperature and time, were based on themodynamic simulations by ThermoCalc® software together with thermal analysis. ThermoCalc® software permitted to obtain the equilibrium phase diagram of the cermets Fe10Al-NbC and Fe10Al-NbC+Fe as a function of the C content. Calculations are based on the Gibbs free energy minimization code and mass conversion rule using the SSOL5 database. The percentage of each of the elements Nb, Fe and Al in the cermet were introduced in the calculation so that increasing the percentage of C decreased proportionately the percentage of other elements.

Thermal analyses were carried out to find out changes in materials during the heating, in particular, phase changes or the presence of a liquid phase. Samples of starting powder and with additions, including the wax used as lubricant for the pressing step (Acrawax C Atomized, Lonza Inc.), were analyzed by Differential Scanning Calorimetry (DSC) in a Netzsch STA 449 C equipment. The analyses were performed under argon up to temperatures of 1300^{o} C, with a heating rate of 10° C/min and cooling rate of 20° C/min. On the other hand, sintered samples were analyzed by Differential Thermal Analysis (DTA) in a SETSYS Evolution equipment (Setaram Instrumentation, France); the tests were performed under argon up to 1490^{o} C with a heating rate of 10° C/min and cooling rate of 20 C/min.

Both DTA and DSC techniques show the phase transformations of materials as a function of temperature variation. The thermal analysis of powders provides a closer approximation to the thermal sintering behavior whereas thermal analysis of the sintered cermets permits a better approach to the equilibrium behavior described in the phase diagrams calculated using ThermoCalc®.

The PS processing was used for producing samples of all compositions prepared. The first step is the blending of powders with 2 wt% Acrawax as lubricant and the powder additions (Fe, C) when required. To ensure homogenization, blending was performed during 2 h in a Turbula® multidirectional mixer. Subsequently the powders were compacted in a uniaxial press at 700 MPa to obtain discs of 16 mm diameter and 3 mm height, and sintered in a high vacuum furnace (10^{-5} mbar) at different temperatures and times, with heating and cooling rates adjusted to 5° C/min.

The consolidation by FAHP was used to produce samples by a faster method, trying to avoid the growth of carbides. Only the starting powder, without additions, was processed by this method. Processing conditions for FAHP were based on those found in the literature for spark plasma sintering of cermets and cemented carbides such as Fe-TiCN [17], NbC-Co [19], WC-Co [20], NbC-WC-Co [21] and Nb carbides and borides [27]. Consolidation by FAHP was conducted in a Gleeble 3800 equipment, in vacuum, at 1100^{o} C with holding time of 15 min, heating and cooling rate of 100 C/min and pressure of 50 MPa applied from 400 °C, temperature at which degassing has already occurred. After consolidation by FAHP the samples were annealed in order to develop a more homogeneous microstructure. The annealing was carried out in argon, with a heating rate of 5^{o} C/min, at 800º C for 20 h. The processing conditions studied for all the materials designed are shown in Table 2.

Table 2. Processing conditions for the materials studied.

Material	**Sintering temperature [ºC] _ time [min]**					
	PS					**FAHP**
	1400_30	1350_30	1300_30	1270_30	1240_60	1100_15
Fe10Al-NbC	X	X	X			X
Fe10Al-NbC+C		X	X			
Fe10Al-NbC+Fe		X	X	X	X	

Fe10Al-NbC+C+Fe		X	X	X	

Sintered samples were characterized by measuring density by He pycnometry and by the Archimedes method, Vickers hardness with 10 kg load (HV10) and by compositional and microstructural analyses by XRD and scanning electron microscopy (SEM) with microanalysis by EDS.

3 Results and discussion

3.1 Characterization of raw material

The chemical composition of starting powders obtained by fluorescence is compared with the composition provided by the supplier in Table 3; other characteristics as density, particle size and carbon percentage of the composite powder as well as the C and Fe additions are shown in Table 4.

Table 3. Chemical composition of the starting powders Fe10Al –NbC (laboratory and supplier analyses).

Method	Chemical Composition (wt. %)						
	Nb	**Fe**	**C**	**Si**	**Al**	**Ti**	**Others**
Fluorescence	40.9	36.1	4.8*	3.4	12.4	2.0	0.4
EDS (Supplier)	40.5	40.3	4.6	2.0	10.0	2.1	0.5

*Measured by LECO.

Table 4. Characteristics of raw materials.

Raw material	Supplier	Experimental data			
		Density (g/cm^3)	**Particle size (μm)**		**C (wt. %)**
Fe10Al-NbC	CBMM	6.2	D_{50}=5.44	D_{90}=11.61	4.8
Fe (Carbonil)	Pometon	7.9	D_{50}=26.42	D_{90}=57.02	0.022
C (grafite)	Istam	2.24*	D_{50}=18*		

*Provided by the supplier.

The SEM images taken in BSE mode (Fig. 1) reveal that Fe10Al-NbC powder particles are constituted by at least three phases, which chemical composition obtained by EDS is shown in the Table 5. The bright phase (1) is identified as niobium carbide containing some Ti; the darkest phase (2) is an alloy containing mainly Fe, Al and Nb, which is the matrix phase agglomerating the disperse phases; and the medium gray phase (3) is a Nb-rich phase containing Fe, Al with a higher concentration of Si than phase (2).

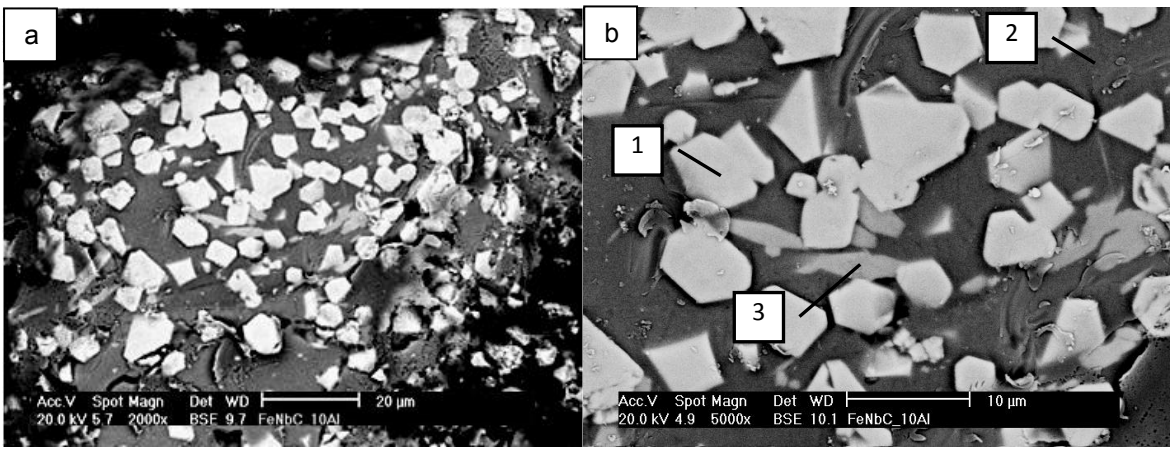

Fig. 1. SEM images (BSE mode) of the raw material Fe10Al-NbC at different magnifications: (a) general view of one particle; (b) detail of the microstructure showing three main phases.

Table 5. Semi quantitative EDS analysis of the phases present in the starting powder Fe10Al-NbC. Composition of the phases marked in Fig. 1b.

Chemical Composition	1 White (NbC)		2 Dark grey (matrix)		3 Medium grey (Intermetallic)	
	wt.%	at.%	wt.%	at.%	wt.%	at.%
C	9.0	41.8	6.7	21.1	1.1	4.9
Nb	84.3	50.6	13.5	5.5	50.3	29.2
Fe	1.4	1.4	53.1	36.0	28.9	28.0
Al	-	-	24.6	34.6	11.2	22.4
Si	-	-	2.1	2.8	7.6	14.5
Ti	5.3	6.2	-	-	0.9	1.0

To identify the phases of the starting powder XRD analysis were performed and the diffraction pattern is shown in the Fig. 2; this figure also contains the diffraction patterns of the sintered samples, but they will be discussed in 3.3.1. From these analyses it seems that the powder Fe10Al-NbC is constituted by stoichiometric NbC (reference code in the PCPDFWIN database 00-038-1364) and intermetallics Fe_3Al (00-050-0955) and $Fe_3Al_{0.7}Si_{0,3}$ (00-045-1204), which have face-centered cubic crystal structure. The phases identified by XRD are partially consistent to those provided by EDS analysis (Table 5). There is no doubt about the presence of NbC carbides, although there is some Ti dissolved in the cubic structure. The matrix contains about 25 wt. % Al, which is slightly higher than the Al content of Fe_3Al, so that it is more consistent to FeAl with a network distorted by Nb or C dissolved. The phase (3) found in the SEM is not identified by XRD. The composition indicates that it could be the intermetallic Fe_2Nb; with hexagonal structure.

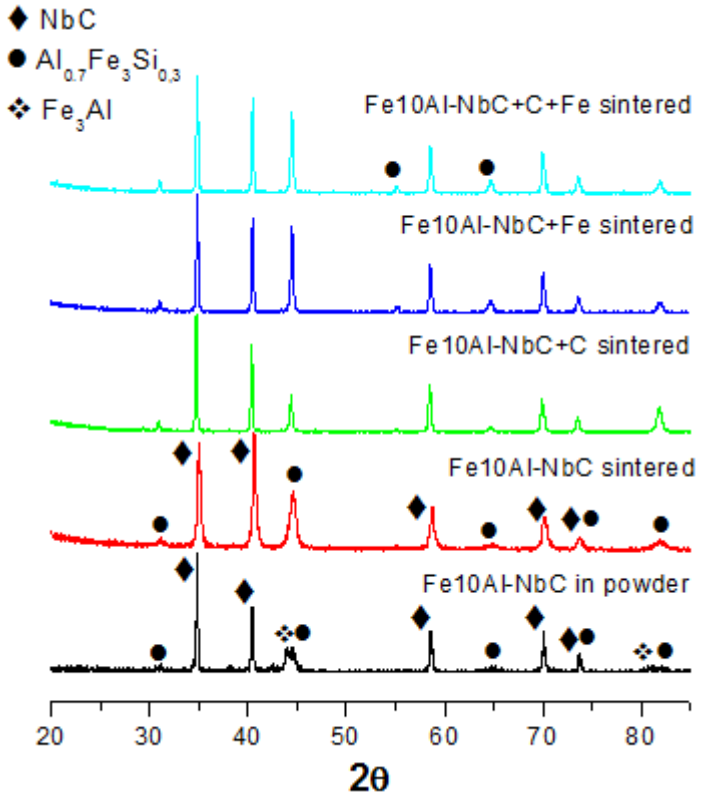

Fig. 2. XRD patterns of the cermets studied processed by pressing and sintering (PS) compared to starting powder Fe10Al-NbC.

The starting powder Fe10Al-NbC and the other compositions prepared according to Table1, were submitted to DSC analyses to find out the reactions during heating, like liquid phase formation, and determine the sintering temperature range; the results are shown in Fig. 3. In all the cases there is an endothermic peak at about 350° C corresponding to the elimination of the lubricant used in the pressing step. The other interesting feature is the fall of the curves (an endothermic reaction) in the last part of the experiments that is associated to the formation of a liquid phase. The highest temperature is for the starting powders without additions (around 1200º C), whereas the lowest temperature (around 1100º C) is for the powder containing both C and Fe.

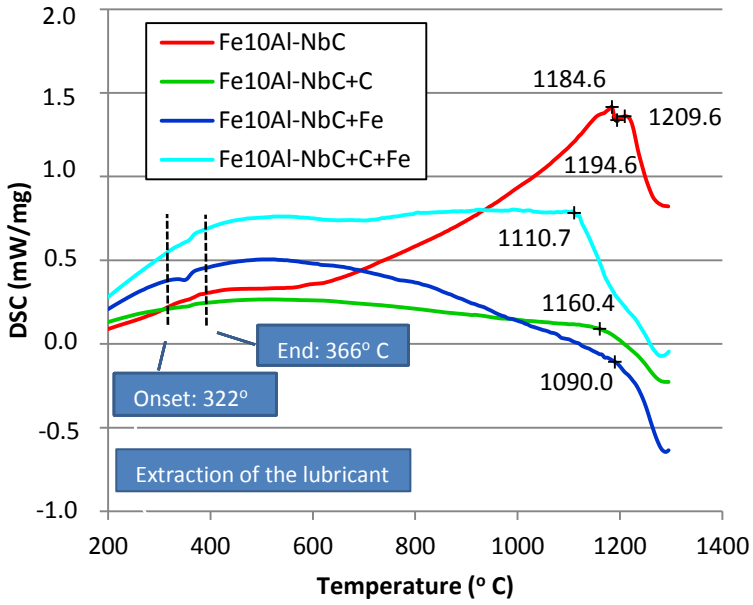

Fig. 3. Thermal analysis DSC of all the compositions studied.

3.2 Thermodynamic simulation by ThermoCalc® and DTA analyses.

The equilibrium phase diagrams were calculated to predict and help to explain the microstructure of the material after sintering; it is also possible to compare the prediction with the microstructure actually observed in the starting powder particles. Two different diagrams were calculated. The first one (Fig. 4) corresponds to the composition of the starting powders with respect to the C content, to compare Fe10Al-NbC and Fe10Al-NbC+C. The second diagram (Fig. 5) corresponds to the composition containing Fe (Fe10Al-NbC+Fe) with respect to the C content, to compare with the composition Fe10Al-NbC+C+Fe.

According to the diagram in Fig. 4 the cermet Fe10Al-NbC at 300º C presents four phases: FeAl, NbC, Nb_5Si_3 and Ti_3SiC_2, and the onset temperature of formation of liquid phase is just below 1200°C. After C addition, the phases predicted at 300° C are FeAl, NbC, Ti_3SiC_2 and Al_8SiC_7, and the onset temperature of formation of liquid phase increases very slightly to just above 1200° C. According to this equilibrium calculation the main elements, i.e. Nb, Fe and Al, appear in the form of NbC and FeAl, whereas the minor elements such as Si and Ti form intermetallic niobium silcides and mixed titanium and silicon carbides, respectively. Prior to the addition of C, aluminum is all in the FeAl phase whereas, when C is added, an aluminum silicon carbide appears to be stable.

It is worth noting that the phases that appear to be more thermodynamically favorable according to the chemical composition of the starting powder do not coincide with the phases actually observed in the powder (Fig. 2). More phases appear to be thermodynamically stable than those actually observed in the powder, which can probably be attributed to the process of production of the powders. Nevertheless it is clear that NbC is present and thermodynamically favorable as well as a matrix phase rich in aluminum.

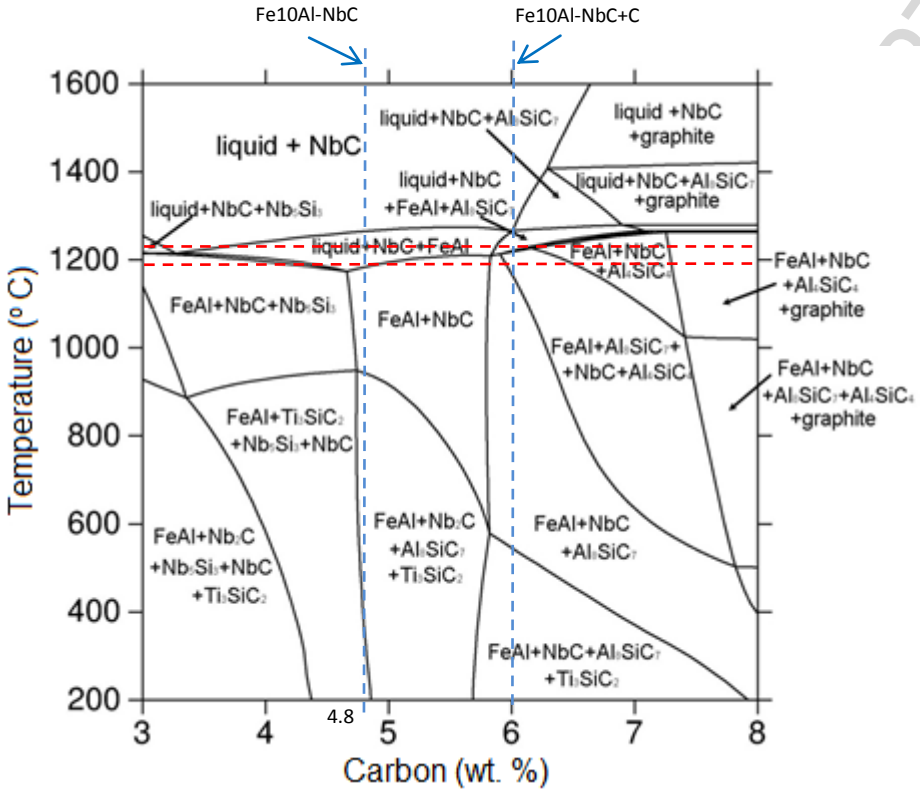

Fig 4. Equilibrium phase diagram calculated by ThermoCalc® of cermet Fe10Al-NbC as a function of the percentage of C.

The cermet Fe10Al-NbC+Fe at 300° C showed the phases FeAl, NbC and Ti_3SiC_2, and the onset temperature of formation of liquid phase increases with respect to the starting composition to about 1280°C (Fig. 5). It is observed that the Fe addition hinders the formation of the phase Nb_5Si_3, which was present in the cermet without Fe addition. By adding C to the Fe10Al-NbC+Fe cermet the Al that was combined only with Fe as FeAl forms mixed carbides of Si, Al. The temperature of formation of the liquid phase is almost the same for the composition containing C.

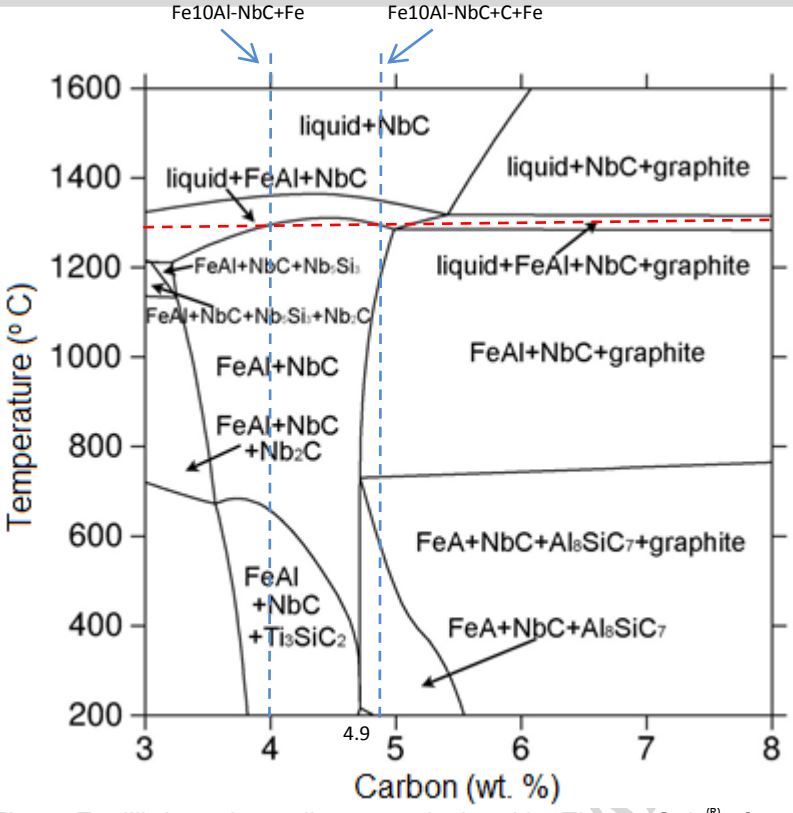

Fig. 5. Equilibrium phase diagram calculated by ThermoCalc® of cermet Fe10Al-NbC+Fe as a function of the percentage of C.

To validate the phase diagrams calculated by ThermoCalc®, sintered samples of the material Fe10Al-NbC were submitted to thermal analysis (DTA). The heating curve (Fig. 6) shows an endothermic peak at 1253.2° C, associated with the formation of a liquid phase which is in close accordance to the phase diagram in Fig. 4, where there is an interval of liquid phase formation between 1180° C and 1260° C, temperature at which the FeAl phase melts. The cooling curve agrees with that transformation temperature, presenting an exothermic peak that should be related to the solidification of the liquid phase. The other small peaks that appear below 1200 °C in the cooling curve could correspond to the solid state reactions predicted in the phase diagram.

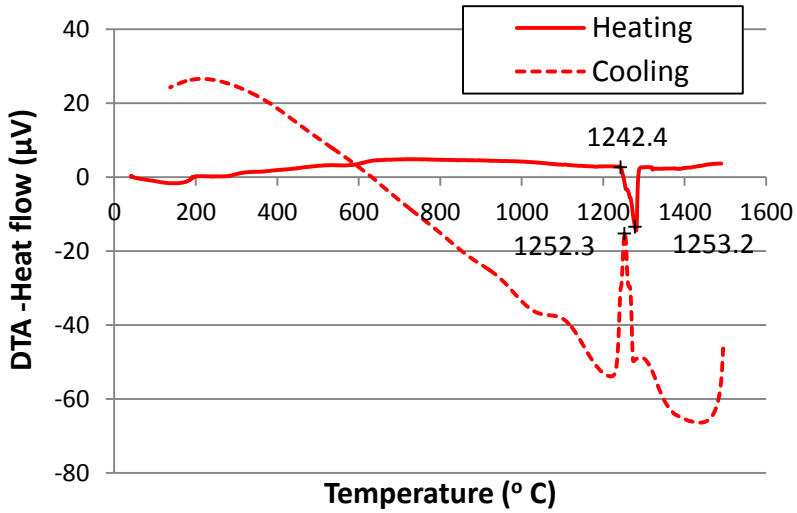

Fig. 6. Thermal analysis DTA of the pressed and sintered cermet Fe10Al-NbC.

3.3 Characterization of consolidated materials

3.3.1 Microstructural characterization

The XRD patterns of the sintered cermets are shown in Fig. 2, compared to the starting powder. All the sintered compositions present two phases: NbC (reference code: 00-038-1364) and $Al_{0.7}Fe_3Si_{0,3}$ (00-045-1204), meaning that some Si diffuses into the Fe_3Al phase during sintering. The minority phases Nb_5Si_3, Ti_3SiC_2 and Al_8SiC_7 that appear to be thermodynamically stable for the compositions of the cermets studied are either not present or cannot be detected by X-ray diffraction.
There is a significant and expected difference in the compositions with Fe additions with respect to the others, which is the higher relative intensity of the peaks corresponding to the $Al_{0.7}Fe_3Si_{0.3}$ phase, due to the higher amount of Fe in global composition.
SEM microstructures of sintered cermets with the highest hardness or density are shown in Fig. 7.

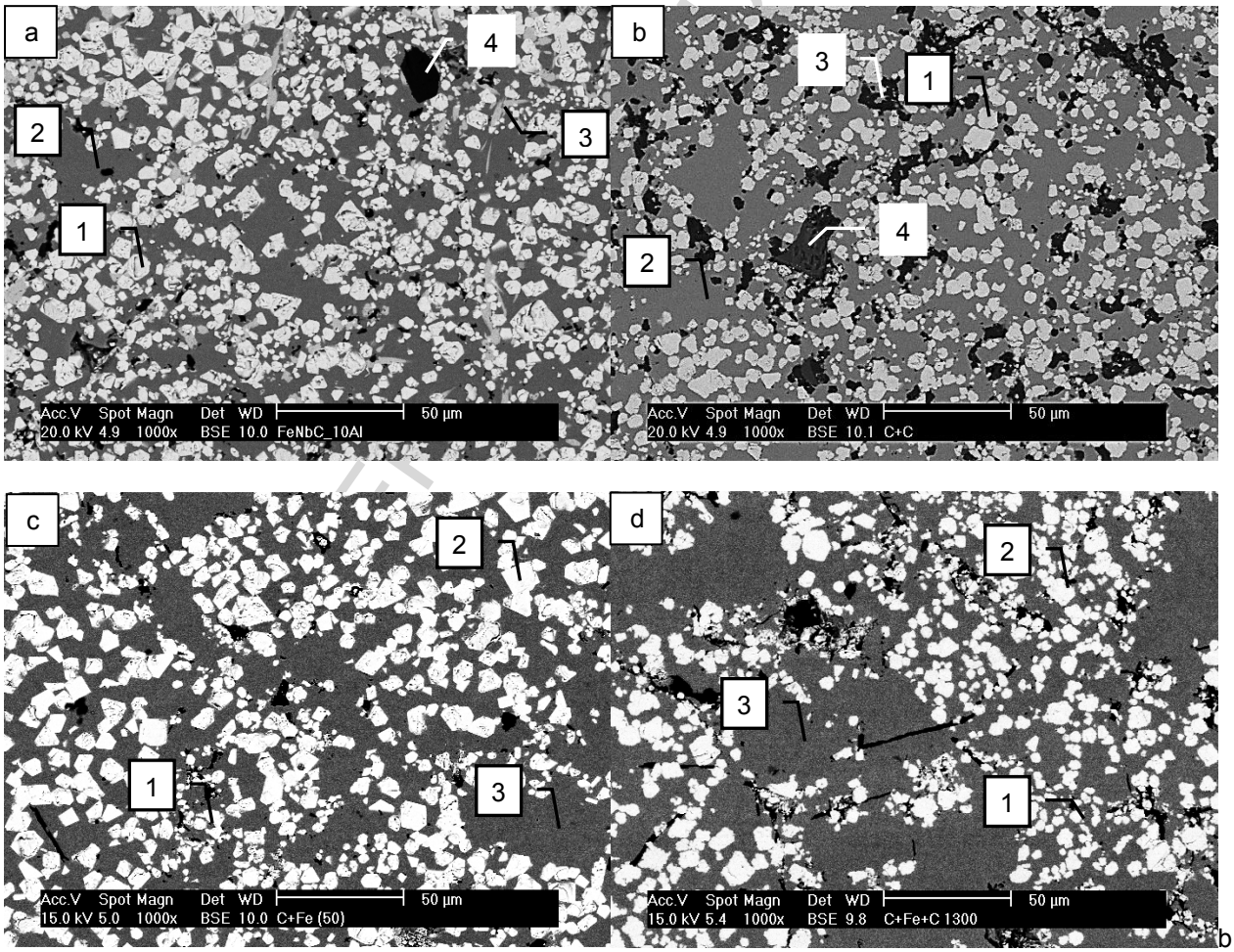

Fig. 7. SEM microstructures (BSE mode) of sintered cermets in different conditions: (a) Fe10Al-NbC, 1400º C, 30min; (b) Fe10Al-NbC+C, 1350º C, 30 min; (c) Fe10Al-NbC+Fe, 1350º C,30 min; (d) Fe10Al-NbC+C+Fe, 1300º C, 30 min.

The numbers in the images show phases which EDS analyses are presented and discussed. The starting sintered material, Fe10Al-NbC (Fig. 7a and Table 6) presents some differences with respect to the microstructure of the powder: (1) the composition of the matrix does not contain Nb and the amount of Fe is higher, agreeing with the phase identified by XRD as matrix, $Al_{0.7}Fe_3Si_{0.3}$; (2) NbC has a higher percentage of carbon indicating the diffusion mechanisms occurring during sintering; (3) a black phase is found

in the sintered material, corresponding to impurities of the starting powder. The medium gray phase is still present in this microstructure, with a slightly different composition than in powder form, containing higher amount of Si and lower amount of Nb.
The cermet Fe10Al-NbC+C (Fig. 7 b and Table 7) shows two main phases, NbC carbides and the matrix phase very similar to that in Fe10Al-NbC, and a dark-contrast phase identified by EDS as complex carbides or oxicarbides; however, the gray intermetallic phase is no longer present. In this case it is also seen the impurities in form of aluminum oxides (black contrast). These phases were not identified by XRD.
Additions of Fe to the cermet (Fe10Al-NbC+Fe, Fe10Al-NbC+Fe+C) resulted in the elimination of gray intermetallic phase and no formation of the black impurity phase (Fig. 7c and d), being pores the black regions in their microstructures. The cermet with both C and Fe addition also presents porosity at the grain boundaries. Table 8 shows the EDS analysis of selected phases in the cermet with Fe addition; the phase analysis of the cermet with both C and Fe addition was omitted, since this is very similar to this with Fe addition.
Table 9 shows the EDS analyses of dark phases in different cermets, where it is clear that these phases are mainly aluminum oxides from the extraction technique used to obtain the powders and it should be removed previously to the processing of the powders.

Table 6. EDS analysis of selected phases in cermet Fe10Al-NbC sintered at 1400^{o} C for 30 min (Fig.7a).

Chemical Composition	1 White (NbC)		2 Dark grey (matrix)		3 Medium grey (Intermetallic)	
	wt.%	at.%	wt.%	at.%	wt.%	at.%
C	10.3	45.4	2.1	7.3	1.2	5.1
Nb	83.0	47.3	-	-	43.8	24.1
Fe	1.4	1.4	73.7	55.6	31.9	29.1
Al	1.4	1.4	18.5	28.8	8.7	16.4
Si	-	-	5.4	8.0	13.3	24.2
Ti	5.3	5.9	0.3	0.3	1.1	1.1

Table 7. EDS analysis of selected phases in cermet Fe10Al-NbC+C sintered at 1350^{o} C for 30 min (Fig.7b).

Chemical Composition	1 White (NbC)		2 Dark grey (matrix)		3 Small black (Al, C, O)	
	wt.%	at.%	wt.%	at.%	wt.%	at.%
C	10.3	45.3	1.4	4.9	12.9	25.9
Nb	81.8	46.3	-	-	7.3	1.9
Fe	1.5	1.4	68.6	50.1	4.1	1.8
Al	-	-	24.4	36.9	69.0	61.8
Si	-	-	5.6	8.1	1.3	1.1
Ti	6.4	7.0	-	-	0.6	0.3
O	-	-	-	-	4.8	7.2

Table 8. EDS analysis of selected phases in cermet Fe10Al-NbC+Fe sintered at 1350° C for 30 min (Fig.7c).

Chemical Composition	1 Small White (NbC)		2 Large White (NbC)		3 Dark grey (matrix)	
	wt.%	at.%	wt.%	at.%	wt.%	at.%
C	10	43.7	12.3	50.2	0.6	2.2
Nb	79.8	45.2	80.9	42.8	1.3	0.6
Fe	1.6	1.6	-	-	74.2	58.4
Al	-	-	-	-	20	32.6
Si	-	-	-	-	3.9	6.2
Ti	8.6	9.5	6.8	7.0	-	-

Table 9. Semi-quantitative phase analysis of the black impurities of different cermets.

Phase	4 Black (Impurities)		4 Large black		4 Black (Impurities)	
Cermet	No add._PS_1400		+ C_PS_1350		No add._FAHP_1100	
Chemical composition	wt.%	at.%	wt.%	at.%	wt.%	at.%
O	30.1	45.2	32.8	49.3	23.9	37.7
Mg	1.1	1.1	-	-	-	-
Al	56.4	50.1	53.0	47.3	59.7	55.8
C	-	-	1.8	1.1	-	-
Ca	3.5	2.1	-	-	4.7	3.0
Ba	4.8	0.8	9.8	1.7	-	-
Ce	4.1	0.7	1.8	0.3	6.6	1.2
Fe	-	-	0.8	0.3	5.1	2.3

The cermet Fe10Al-NbC was also processed by FAHP and then annealed to homogenize microstructure. SEM images of as-sintered and annealed conditions are shown in Fig. 8, where the same phases are visible, and the compositions shown in Table 10. Some differences are observed in this cermet with respect to the cermet processed by PS (Fig. 7a and Table 6): the carbide NbC contains less amount of carbon and the matrix more aluminum and carbon with respect to the same phases in cermet by PS. This can be due to the lower temperature and processing time in the FAHP process, which hinders the diffusion mechanisms. The intermetallic phase and black impurities have similar composition in both cermets with different processing.

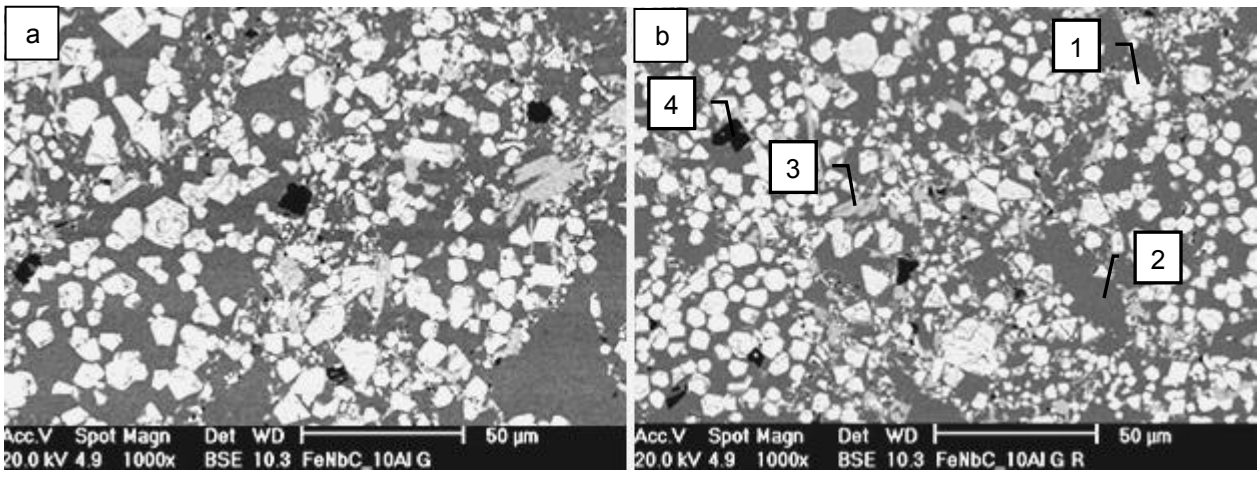

Fig. 8. Cermets Fe10Al-NbC without addition, 1000x, BSE: (a) consolidated by FAHP; (b) consolidated by FAHP and annealed.

Table 10. EDS analysis of selected phases in cermet Fe10Al-NbC consolidated by FAHP and annealed (Fig.8).

Chemical composition	1 White (NbC)		2 Dark grey (matrix)		3 Medium grey (Intermetallic)	
	wt.%	at.%	wt.%	at.%	wt.%	at.%
C	8.9	41.3	3.9	12.0	-	-
Nb	83.7	50.2	-	-	50.6	30.4
Fe	0.9	0.9	63.8	43.1	28.9	28.9
Al	-	-	27.2	38.0	10.3	21.3
Si	-	-	5.1	6.9	9.1	18.1
Ti	6.5	7.6	-	-	1.1	1.3

3.3.2 Density and hardness

The density of samples were measured by Archimedes method and by He pycnometer and presented as relative densities, calculated as a percentage of the theoretical densities. The Table 11 presents the theoretical densities calculated from the rule of mixtures based on the densities of the raw materials, obtained by pycnometry or provided by suppliers (Table 4).

Table 11. Theoretical density of the powder and mixtures.

Cermet	Th. Density (g/cm^3)
Fe10Al-NbC	6,242
Fe10Al-NbC+C	6,122
Fe10Al-NbC+Fe	6,487
Fe10Al-NbC+C+Fe	6,352

The relative density of cermets calculated from Archimedes data are shown in Table 12, whereas Table 13 shows the relative density from pycnometry data. The first idea to explain from these data is the fact that some values of relative density are higher than 100. This is due to the reactions occurred during sintering, that provide phases different than those on the starting material, so that the theoretical density obtained by the rule of mixtures is not the best reference for relative density, or for obtaining data of porosity from the values of density. However, by comparison of data in tables 12 and 13, some conclusions can be extracted: (1) the density increases with the sintering temperature, due to the increasing amount of liquid phase; (2) most of the porosity should be open porosity; (3) except the base material (Fe10Al-NbC), the other compositions do not reach full density in the conditions studied, due to the remaining large pores and the presence of phases of low density present in the microstructure (oxides and oxicarbides, Table 7). The compositions with Fe addition (Fe10Al-NbC+Fe, Fe10Al-NbC+C+Fe) require lower sintering temperature as it was observed the formation of large amount of liquid phase, evidenced by the dimensional deformation of samples when sintering temperature was higher than 1270ºC for the addition of Fe and 1240ºC for the addition of Fe and C. This behavior is attributed to the heterogeneity of the green compacts, formed by blending of Fe10Al-NbC powders and Fe and graphite powders. In those conditions the phase diagrams calculated by ThermoCalc®, in which the formation of liquid phase appears at temperatures higher than in cermets without Fe addition, do not give the correct picture; instead, the DSC experiments (Fig. 3) explain better the behavior, as they provide the starting temperatures of liquid phase formation of the green compacts. Even with the

formation of liquid phase, the density of Fe10Al-NbC+Fe and Fe10Al-NbC+C+Fe is low probably due to the need of higher sintering time.

Table 12. Relative density from Archimedes measurements of materials sintered in different conditions.

Cermet	Relative density (% th.) - Archimedes					
	PS					FAHP
	1400_30	1350_30	1300_30	1270_30	1240_60	1100_15
Fe10Al-NbC	**101.8**	90.0	93.5			100.7
Fe10Al-NbC+C		**91.5**	88.5			
Fe10Al-NbC+Fe		**95.9**	86.0	77.8	73.6	
Fe10Al-NbC+C+Fe			**90.3**	88.3	**96.1**	

Table 13. Relative density from pycnometry measurements of the materials sintered in different conditions.

Cermet	Relative density (%th) - pycnometry					
	PS					FAHP
	1400_30	1350_30	1300_30	1270_30	1240_60	1100_15
Fe10Al-NbC	106.5	101.4	99.2			99.9
Fe10Al-NbC+C		102.0	102.3			
Fe10Al-NbC+Fe		101.3	102	103.4	103.1	
Fe10Al-NbC+C+Fe			104.1	105.8	103.7	

The values of hardness (HV10) of sintered samples are shown in Table 14. The highest values are obtained for samples processed by FAHP in both as sintered and annealed conditions. These values are comparable to those obtained in the study of Esteban et al. [22]. The hardness of PS samples follow the same trend than density, that is, increases with sintering temperature, but the highest values are for the composition Fe10Al-NbC, without Fe and C additions. Taking into account the expected amount of phases from the composition of the cermets, there should be about 42 wt. % NbC in the composite Fe10Al-NbC (considering that all the C present is combined with NbC); 45.6 wt. % NbC in the cermet with C addition; 34.5 wt. % NbC and 38.3 wt. % NbC for the cermets Fe10Al-NbC+Fe and Fe10Al-NbC+C+Fe respectively. Then, the lower hardness of cermets with Fe additions is attributed to the lower amount of hard phase, whereas the low hardness of Fe10Al-NbC+C, that should contain higher amount of NbC precipitates is due to the heterogeneous diffusion of carbon and the formation of oxides and oxicarbides throughout the microstructure (Fig. 7b).

Table 14. Hardness (HV10) of the materials sintered in different conditions.

Cermet	Hardness (HV10)						
	PS - Temperature (^{o}C)_Time (min)					FAHP	FAHP and Annealed
	1400_30	1350_30	1300_30	1270_30	1240_60	1100_15	1100_15
Fe10Al-NbC	508.5±44.61	524.8±29.16	431.6±39.39			620.8±15.59	693.8±20.80
Fe10Al-NbC +C		363.2±24.70	274.4±24.70				
Fe10Al-NbC +Fe		505.4±59.03	268.2±26.74	112.5±10.33	92.5±6.67		
Fe10Al-NbC +C+Fe			218.5±22.63	192.8±8.86	119.2±11.27		

Comparing the hardness of cermet Fe10Al-NbC processed by PS and FAHP in as-sintered and annealed conditions, the latter presents the higher values. This is attributed to the high densification and more homogeneous microstructure.
The highest values of hardness achieved in these cermets are about 700 HV10 in the cermet Fe10Al-NbC processed by FAHP and annealed. This hardness is low compared to

some studies about Fe-based cermets with NbC as that about mechanosynthesis (1224HV) [21] or compared to other compositions like M2-TiCN (1336 HV) [23], but is similar or higher than the hardness achieved in most works related to Fe-NbC system (286 - 800HV) [17], [20], [22], [28]. It is noteworthy that this study did not use any method to decrease the particle size or to improve the dispersion of the carbides in the matrix.

4. Conclusions

The starting material of this work is a composite powder obtained by an extraction method from Nb ores to produce particles containing NbC precipitates in a Fe-rich matrix. The processing of this powder is studied to obtain a Fe matrix cermet: the microstructure and some properties of sintered cermets are present and some conclusions are as follow:

- Three main phases are identified in the composite powders (NbC, FeAl and $Fe_3Al_{0.7}Si_{0.3}$), which are also observed with some variations in sintered materials due to diffusion promoted by sintering. The main changes are essentially the diffusion of C from FeAl to NbC.
- The addition of C to the base material does not improve the processing, nor the microstructure and properties. Complex carbides and oxicarbides are observed in the microstructure, which lower the densification and hardness.
- Phase diagrams of the system studied were calculated by ThermoCalc®. DTA analysis of sintered material confirms that the prediction is accurate. However the diagrams are not useful to predict the sintering behavior due to the heterogeneous blending.
- DSC analyses provided the temperature of liquid phase formation of all the compositions studied. The highest is for base material (Fe10Al-NbC) at about 1200ºC, followed by Fe10Al-NbC+C, Fe10Al-NbC+Fe, Fe10Al-NbC+C+Fe (1110 ºC). This is in accordance to the observed behavior of materials during sintering.
- Cermets with Fe additions only present two phases (NbC and FeAl), impurities and intermetallics are not found.
- Processing by FAHP resulted in higher hardness than PS processing in the conditions studied, reaching 700 HV10.

Acknowledgements

The authors would like to acknowledge financial support from FAPESC and CAPES to the PhD student, the Universidad Carlos III de Madrid for the research abroad, the CBMM for donation of the cermet and the research institution IMDEA for carrying out the processing by FAHP. The financial support from the Spanish government through the R&D project MAT2012-38650-C02-01 is also acknowledged.

References

[1] ASM International. Powder Metallurgy Cermets and Cemented Carbides. In: ASM ASM International, editors. Handbook Powder Metal Technologies and Applications, E-Publishing; 1988, 2312–55.

[2] Eckert J. Niobium Compounds and Alloys. Int J Refract Met Hard Mater 1994;12:335–40.

[3] Official Journal of the European Union, “Commission Regulation (EC) No 790/2009: amending, for the purposes of its adaptation to technical and scientific progress,

Regulation (EC) No 1272/2008 of the European Parliament and of the Council on classification, labelling and packaging of substances," Official Journal of the European Union 5.9.2009, L235/1, http://eur-lex.europa.eu/LexUriServ/LexUriServ.do?uri=OJ:L:2009:235:0001:0439:en:PDF(accessed March 15, 2014).

[4] Services, U.S. Dept. of Health and Human, " 12th Report on Carcinogens - Cobalt-tungsten carbide: powders and hard metals -Public Health Service," National Toxicology Program 2011, http://ntp.niehs.nih.gov/ntp/roc/twelfth/profiles/CobaltTungstenCarbide.pdf (accessed March 15, 2014).

[5] P. Alvaredo, S. A. Tsipas, E. Gordo. Influence of carbon content on the sinterability of an FeCr matrix cermet reinforced with TiCN. Int. Journal of Refractory Metals and Hard Materials 36 (2013) 283–288.

[6] Umanskii AP. Titanium Carbonitride Composite with Iron — Chromium Binder. Powder Metall Met Ceram 2001; 40:637–40.

[7] Klaasen H, Kübarsepp J, Roosaar T, Viljus M, Traksmaa R. Adhesive wear performance of hardmetals and cermets. Wear 2010; 268:1122–8.

[8] Canteli JA, Cantero JL, Marín NC, Gómez B, Gordo E, Miguélez MH. Cutting performance of TiCN–HSS cermet in dry machining. J Mater Process Technol 2010; 210:122–8.

[9] Woydt M, Mohrbacher H. Tribological plofile of binderless niobium carbide. In: Singh D, Salem J, editors. Mechanical properties and performance of engineering cerâmicas and composites VIII, New Jersey: John Wiley and Sons Inc; 2013, 189–93.

[10] Rahimi Dizaji V, Rahmani M, Faghihi Sani M, Nemati Z, Akbari J. Microstructure and cutting performance investigation of Ti(C, N)-based cermets containing various types of secondary carbides. Int J Mach Tools Manuf 2007; 47:768–772.

[11] Li Y, Liu N, Zhang X, Rong C. Effect of WC content on the microstructure and mechanical properties of (Ti,W)(C,N)-Co cermets. Int J Refract Met Hard Mater 2008; 26:33–40.

[12] Davis JR. Cemented Carbides. In: ASM International, editors. Tool Materials, 1995, 36–59.

[13] Toth LE. Transition metal carbides and nitrides. Refractory Materials. In: Academic Press, editors. A Series of Monographs, New York; 1971, 1–26.

[14] Araújo Filho OO de, Neves MDM das, Gonzalez CH, Urtiga Filho SL, Ambrozio Filho F. Processing of AISI M2 HSS with Addition of NbC by Mechanical Alloying Using two Different Types of Attritor Mills. Mater Sci Forum 2010; 660-661:17–22.

[15] Woydt M. Tribological Profile of Binderless and Cobalt Bonded Niobium Carbide. In: EPMA, editor. Proceedings of the Euro PM2013 Conference 2013.

[16] Gordo E, Velasco F, Antón N, Torralba JM. Wear mechanisms in high speed steel reinforced with (NbC) p and (TaC)p MMCs. Wear 2000; 239: 251–9.

[17] Gordo E, Gómez B, González R, Ruiz-Navas EM. Study for the Development of Fe-NbC Composites by Advanced PM Techniques. Mater Sci Forum 2007; 536:637–40.

[18] Klein AN, Martinelli AE, Nascimento M, Candice B, Guedes DF. Microstructural characterizattion of conventionally and plasma- sintered Fe-NbC and Fe-TaC Composites. Int J Powder Metall 2011; 47:29–37.

[19] Martinelli AE, Paulo DSA, Nascimento RM, Távora MP, Gomes UU, Alves Jr. C. Dilatometric behavior and microstructure of sintered Fe–NbC and Fe–TaC composites. J Mater Sci 2006; 42:314–9.

[20] Zhong L, Xu Y, Ye F. In Situ NbC Particulate-Reinforced Iron Matrix Composite: Microstructure and Abrasive Wear Characteristics. Tribol Lett 2012; 47:253–9.

[21] Yazovskikh KA, Lomayeva SF. Mechanosynthesis of Fe–NbC nanocomposite. J Alloys Compd 2013; 2012–4.

[22] Esteban PG, Gordo E. Development of Fe–NbC cermet from powder obtained by self-propagating high temperature synthesis. Powder Metall 2006; 49:153–9.

[23] Alvaredo P, Gordo E, Van der Biest O, Vanmeensel K. Microstructural development and mechanical properties of iron based cermets processed by pressureless and spark plasma sintering. Mater Sci Eng A 2012; 538:28–34.

[24] Huang SG, Van der Biest O, Li L, Vleugels J. Properties of NbC–Co cermets obtained by spark plasma sintering. Mater Lett 2007; 61:574–7.

[25] Zhao S, Song X, Wei C, Zhang L, Liu X, Zhang J. Effects of WC particle size on densification and properties of spark plasma sintered WC–Co cermet. Int J Refract Met Hard Mater 2009; 27:1014–8.

[26] Huang SG, Liu RL, Li L, Van der Biest O, Vleugels J. NbC as grain growth inhibitor and carbide in WC–Co hardmetals. Int J Refract Met Hard Mater 2008; 26:389–95.

[27] Tsuchida T, Kakuta T. Fabrication of SPS compacts from NbC–NbB2 powder mixtures synthesized by the MA–SHS in air process. J Alloys Compd 2006; 415:156–61.

[28] Gordo E, Oliva A, Torralba JM. Desarrollo de materiales compuestos tipo Cermet de matriz Fe. Bol Soc española cerámica y Vidrio 2004; 43:416–9.

Highlights

- A cermet Fe10Al-NbC was obtained by conventional powder metallurgy and FAHP.
- Raw material is an in-situ NbC composite powder produced from Nb ore.
- Phase diagrams were calculated by ThermoCalc® to explain the microstructure.
- The microstructure of sintered cermet contains NbC particles in a Fe-Al matrix.
- Properties of different compositions produced by PM and FAHP are compared.